

# Cosmological Constraints from Type Ia Supernovae Peculiar Velocity Measurements

C. Gordon, K. Land, and A. Slosar  
*Oxford Astrophysics, Physics, DWB, Keble Road, Oxford, OX1 3RH, UK*

We detect the correlated peculiar velocities of nearby type Ia supernovae (SNe), while highlighting an error in some of the literature. We find  $\sigma_8 = 0.79 \pm 0.22$  from SNe, and examine the potential of this method to constrain cosmological parameters in the future. We demonstrate that a survey of 300 low- $z$  SNe (such as the nearby SNfactory) will underestimate the errors on  $w$  by  $\sim 35\%$  if the coherent peculiar velocities are not included.

The first compelling evidence that the Universe is undergoing a period of accelerated expansion was provided by observations of Type Ia supernovae (SNe) [1, 2]. The data from many current [3, 4, 5] and near future [6, 7, 8, 9] surveys should eventually constrain the effective dark energy equation of state to better than 10%.

Density inhomogeneities cause the SNe to deviate from the Hubble flow, as gravitational instability leads to matter flowing out of under-densities and into over-densities. These “peculiar velocities” (PVs) lead to an increased scatter in the Hubble diagram, of which several studies have been made [10, 11, 12, 13, 14, 15, 16, 17, 18, 19, 20, 21, 22]. When combining low and high redshift SNe in order to estimate the properties of the dark energy, the velocity contributions are usually modeled as a Gaussian noise term which is uncorrelated between different SNe. However, as recently emphasized [23], in the limit of low redshift  $z \lesssim 0.1$  and large sample size, the correlations between SNe PVs contribute significantly to the overall error budget. In this letter we investigate the effect of incorporating these correlations using the largest available low redshift compilation [17].

## I. PECULIAR VELOCITY COVARIANCE

The luminosity distance,  $d_L$ , to a SN at redshift  $z$ , is defined such that  $\mathcal{F} = \frac{\mathcal{L}}{4\pi d_L^2}$  where  $\mathcal{F}$  is the observed flux and  $\mathcal{L}$  is the SN’s intrinsic luminosity. Astronomers use magnitudes, which are related to the luminosity distance (in megaparsec) by

$$\mu \equiv m - M = 5 \log_{10} d_L + 25, \quad (1)$$

where  $m$  and  $M$  are the apparent and absolute magnitudes respectively. In the context of SNe,  $M$  is a “nuisance parameter” which is degenerate with  $\log(H_0)$  and can be marginalised over. For a Friedmann-Robertson-Walker Universe the predicted luminosity distance is given by

$$d_L(z) = (1+z) \int_0^z \frac{dz'}{H(z')} \quad (2)$$

in speed of light units, where  $H$  is the Hubble parameter. In the limit of low redshift this reduces to  $d_L \approx z/H_0$ .

Assuming a flat Universe (as we shall do throughout this letter), the effect of peculiar velocities leads to a

perturbation in the luminosity distance ( $\delta d_L$ ) given by [23, 24, 25, 26, 27]

$$\frac{\delta d_L}{d_L} = \hat{\mathbf{r}} \cdot \left( \mathbf{v} - \frac{(1+z)^2}{H(z) d_L} [\mathbf{v} - \mathbf{v}_O] \right) \quad (3)$$

where  $\mathbf{r}$  is the position of the SN, and  $\mathbf{v}_O$  and  $\mathbf{v}$  are the peculiar velocities of the observer and SN respectively. Using the Cosmic Microwave Background dipole we can very accurately correct for  $\mathbf{v}_O$ . This demonstrates how a SNe survey that measures  $\mu$  and  $z$  can estimate the projected PV field. We now relate this to the cosmology.

The projected velocity correlation function,  $\xi(\mathbf{r}_i, \mathbf{r}_j) \equiv \langle (\mathbf{v}(\mathbf{r}_i) \cdot \hat{\mathbf{r}}_i)(\mathbf{v}(\mathbf{r}_j) \cdot \hat{\mathbf{r}}_j) \rangle$ , must be rotationally invariant, and therefore it can be decomposed into a parallel and perpendicular components [28, 29, 30] :

$$\xi(\mathbf{r}_i, \mathbf{r}_j) = \sin \theta_i \sin \theta_j \xi_{\perp}(r, z_i, z_j) + \cos \theta_i \cos \theta_j \xi_{\parallel}(r, z_i, z_j)$$

where  $\mathbf{r}_{ij} \equiv \mathbf{r}_i - \mathbf{r}_j$ ,  $r = |\mathbf{r}_{ij}|$ ,  $\cos \theta_i \equiv \hat{\mathbf{r}}_i \cdot \hat{\mathbf{r}}_{ij}$ , and  $\cos \theta_j \equiv \hat{\mathbf{r}}_j \cdot \hat{\mathbf{r}}_{ij}$ . In linear theory, these are given by [28, 29, 30]:

$$\xi_{\parallel, \perp} = D'(z_i) D'(z_j) \int_0^\infty \frac{dk}{2\pi^2} P(k) K_{\parallel, \perp}(kr) \quad (4)$$

where for an arbitrary variable  $x$ ,  $K_{\parallel}(x) \equiv j_0(x) - \frac{2j_1(x)}{x}$ ,  $K_{\perp}(x) \equiv j_1(x)/x$ .  $D(z)$  is the growth function, and derivatives are with respect to conformal time.  $P(k)$  is the matter power spectrum. This corrects the formulae used in [31, 32], see the Appendix for details.

The above estimate of  $\xi(\mathbf{r}_i, \mathbf{r}_j)$  is based on linear theory. On scales smaller than about  $10h^{-1}\text{Mpc}$  nonlinear contributions become important. These are usually modeled as an uncorrelated term which is independent of redshift, often set to  $\sigma_v \sim 300 \text{ km/s}$ . Comparison with numerical simulations [33] has confirmed that this is an effective way of accounting for the nonlinearities. Other random errors that are usually considered are those from the lightcurve fitting ( $\mu_{\text{err}}$ ), and intrinsic magnitude scatter ( $\sigma_m$ ) found to be  $\sim 0.08$  in the case of [17]. It is just these three errors that are usually included in the analysis of SNe.

In Fig. 1 we compare the covariance of  $\delta d_L/d_L$  from peculiar velocities for a pair of SN

$$C_v(i, j) = \left( 1 - \frac{(1+z)^2}{H d_L} \right)_i \left( 1 - \frac{(1+z)^2}{H d_L} \right)_j \xi(\mathbf{r}_i, \mathbf{r}_j) \quad (5)$$

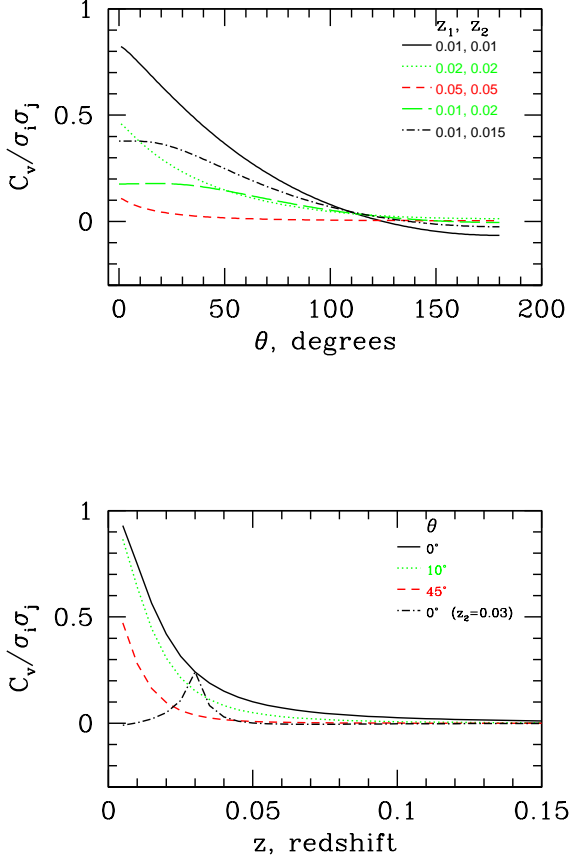


FIG. 1: The ratio of the covariance from peculiar velocities  $C_v$ , compared to the random errors  $\sigma$ , for a pair of supernovae, over a range of angular separations. In the upper panel we vary the separation on the sky,  $\theta$ . In the lower panel we vary the redshift, with them both at the same  $z$  or with one supernovae fixed at  $z = 0.03$  (dash-dot).

to the standard uncorrelated random errors given by

$$\sigma(i)^2 = \left( \frac{\ln(10)}{5} \right)^2 (\sigma_m^2 + \mu_{\text{err}}(i)^2) + \left( 1 - \frac{(1+z)^2}{H d_L} \right)_i^2 \sigma_v^2 \quad (6)$$

with  $\{\Omega_m, \Omega_b, h, n_s, w, \sigma_8\} = \{0.3, 0.05, 0.7, 0.96, -1, 0.85\}$  and  $\{\mu_{\text{err}}, \sigma_m, \sigma_v\} = \{0.1, 0.08, 300\}$ . We see that the PV covariance is comparable with the uncorrelated errors for low- $z$ , and we note that the correlated errors become more significant the larger the dataset.

## II. CONSTRAINTS FROM CURRENT DATA

A uncorrelated-error-only analysis of SNe allows one to constrain the cosmological parameters through the Hubble parameter in (2). Namely  $\Omega_m$  and  $w$ , for a flat

Universe. However, by fitting for the PV covariance we probe the matter power spectrum and can therefore constrain further parameters such as  $\Omega_b, H_0, n_s, \sigma_8$ , where these have their usual meaning. In the following analysis we also allow the SNe ‘‘nuisance’’ parameters  $M, \sigma_m, \sigma_v$  to vary. These are often set to fixed values, however marginalizing over them allows a better estimate of the uncertainty in the other parameters. The weighted integration of the matter power spectrum in Eq. (4) has similar weights to those used in evaluating  $\sigma_8$ . Therefore, the higher  $\sigma_8$ , the stronger the correlations between the projected velocities, obeying  $C_v \propto \sigma_8^2$  for the other parameters fixed.

We analyse nearby supernovae ( $z \leq 0.12$ ) from [17] who find improved luminosity distances to 133 supernovae from a multicolour light curve method. Following [17] we exclude 9 supernovae from the set. These are supernovae that are unsuitable due to bad lightcurve fits, those who have their first observation more than 20 days after maximum light, are hosted in galaxies with excessive extinction ( $A_V^0 > 2.0$  mag) and one outlier (SN1999e). This leaves 124 supernovae  $z \in [0.0023, 0.12]$ , which have an average separation of  $\bar{r} = 108 h^{-1}\text{Mpc}$ , a mean redshift  $\bar{z} = 0.024$ , and herein we refer to this dataset as our ‘‘low- $z$ ’’ SNe.

The likelihood is given by

$$\mathcal{L} \propto |\Sigma|^{-1/2} e^{-\frac{1}{2} x^T \Sigma^{-1} x}$$

where  $\Sigma(i, j) = C_v(i, j) + \sigma(i)^2 \delta_{ij}$  and  $x = [d_L^{obs} - d_L(z)]/d_L(z)$  with  $d_L^{obs}$  given by Eq. (1), and  $d_L(z)$  by Eq. (2). The matter power spectrum can be evaluated either numerically (e.g. CAMB [34]) or using analytical approximations [35]. We assume a flat Universe with a cosmological constant ( $w = -1$ ), a Big Bang Nucleosynthesis (BBN) prior  $\Omega_b h^2 \sim \mathcal{N}(0.0214, 0.002)$  [36], and a Hubble Space Telescope (HST) prior  $h \sim \mathcal{N}(0.72, 0.08)$  [37]. These two priors remove models that are wildly at odds with standard cosmological probes, but do not unduly bias results towards standard cosmology. The likelihood has almost negligible dependence on  $n_s$ , and to keep it in a range consistent with CMB and large scale structure estimates we give it a uniform prior  $n \in [-0.9, 1.1]$ . The other parameters are all given broad uniform priors. We use the standard Markov Chain Monte Carlo (MCMC) method to generate samples from the posterior distribution of the parameters [38]. Convergence was checked using multiple chains with different starting positions, and also the  $R - 1$  statistic [39]. We also checked that the estimated posterior distributions reduced to the prior distributions when no data was used [42]. All the analysis was checked with two completely independent codes and MCMC chains.

The low- $z$  results are given in row A of Table I. As a non-zero  $\sigma_8$  is needed for the velocity correlations, these results indicate the correlations are detected at the  $3.6\sigma$  level. We also perform the MCMC runs without including the PV covariance matrix  $C_v$ , and we find  $-2 \ln \mathcal{L}_{\text{max}}$  (where  $\mathcal{L}$  is the likelihood) increases by 19.3. As the

likelihood no longer depends on  $\{\sigma_8, \Omega_b, h, n_s\}$  we have effectively removed four parameters.

When estimating the cosmological parameters from SNe, a low redshift cut is usually imposed, to reduce the effects of the PVs. For example in [40], their SNe dataset have 192 SNe with  $z \in [0.016, 1.76]$  and a mean redshift of  $\bar{z} = 0.48$ . Herein we refer to this dataset as our “high- $z$ ” SNe. Our MCMC results for just this data (without including PVs) are shown in row B of Table I. Although we marginalize over the SNe parameters  $\{M, \sigma_v, \sigma_s\}$ , our constraints on  $\Omega_m$  are still in excellent agreement with those obtained in [40].

We now combine the low- $z$  and the high- $z$  datasets, to make an “all- $z$ ” dataset. We used the overlapping SNe in the two datasets to estimate a small normalizing offset to the magnitudes from the latter data set, (the extra magnitude error is negligibly small). The same procedure was used by [40] in constructing their dataset. After eliminating duplicated SNe, our combined all- $z$  dataset has 271 SNe with  $z \in [0.0023, 1.76]$ , and  $\bar{z} = 0.35$ . Our all- $z$  results are given in row C of Table I. The constraints on  $\sigma_8$  broaden slightly due to a mild degeneracy between  $\sigma_8$  and  $\Omega_m$  which is broken by the addition of the higher  $z$  SNe, but pushes  $\sigma_8$  to the region of higher uncertainty. The increase in the minimum of  $-2 \ln \mathcal{L}$ , when  $\sigma_8$  is set to zero, is now 16.4.

One the main aims of cosmology is to test the cosmological constant prediction  $w = -1$ . Due to a degeneracy between  $w$  and  $\Omega_m$ , it is necessary to combine the SNe with another data source. Here we use the WMAP CMB data [41]. We continue to assume a flat Universe, and we now allow  $w$  to be a free parameter. The results are given in rows D to H of Table I and in Fig. 2. As can be seen by comparing rows D and E, if a redshift cutoff of  $z \geq 0.016$  is made, then current data has a systematic error of  $\delta w = 0.02$  when PVs are not included. This is several times smaller than the statistical error of  $\delta w = 0.08$ . However, comparing rows F and G, shows that if no redshift cutoff is made, neglecting the correlated PVs results in a systematic error of  $\delta w = 0.07$  which is about as large as the statistical error.

### III. FORECASTS

We now consider the relevance of peculiar velocities to future supernovae surveys, using a Fisher matrix analysis. The Fisher (information) matrix probes the ability of an experiment to constrain parameters, by looking at the dependence of the likelihood:  $F_{\alpha\beta} \equiv -\left\langle \frac{\partial^2 \ln \mathcal{L}}{\partial p_\alpha \partial p_\beta} \right\rangle$

$$F_{\alpha\beta} = \mathbf{d}_{,\alpha} \mathbf{C}^{-1} \mathbf{d}^T_{,\beta} + \frac{1}{2} \text{Tr} (\mathbf{C}^{-1} \mathbf{C}_{,\alpha} \mathbf{C}^{-1} \mathbf{C}_{,\beta}) \quad (7)$$

Often the second term is ignored, however we find that this approximation is no longer valid when including PVs. Unmarginalised  $1\sigma$  errors on parameter  $p_\alpha$  are given by  $\sqrt{(1/F_{\alpha\alpha})}$ , and the equivalent marginalised errors by  $\sqrt{\{F^{-1}\}_{\alpha\alpha}}$ . Generally, the inverted Fisher matrix  $F^{-1}$

provides the expected covariance matrix for the parameters.

We consider two future supernova experiments that aim to detect high and low-redshift supernovae respectively: the Supernova/Acceleration Probe (SNAP, [9]), and the Nearby Supernova Factory (SNfactory, [6]). The baseline SNfactory program is to obtain spectrophotometric lightcurves for SNe in the redshift range  $0.03 < z < 0.08$ , with the assumption that these SNe are far enough away for correlated peculiar velocities to not contribute significantly to the error budget. However, in Fig 1 we can see the contribution of correlated PVs is not irrelevant for  $z \sim 0.03$ , and as the number of SNe increases the overall uncertainty from random errors (such as intrinsic magnitude scatter and instrumental noise) gets beaten down by a  $1/\sqrt{N}$  factor, while the correlated errors from coherent peculiar velocities do not. Thus at any redshift, these peculiar velocity errors will begin to dominate for some large number of SNe. We investigate the situation for the SNfactory by considering 300 SNe randomly distributed over a rectangular area of 10,000 sq degrees, and redshifts  $0.03 < z < 0.08$ . We also include high- $z$  from a SNAP-like survey, and model this as 2000 SNe randomly distributed over 10 sq degrees with  $0.2 < z < 1.7$ , and we assume PVs are irrelevant for these SNe. We take our fiducial model to be a flat  $\Lambda$ CDM cosmology with  $\Omega_m=0.3$ ,  $\Omega_b = 0.05$ ,  $h = 0.7$ ,  $n_s = 0.96$ ,  $w = -1$ ,  $\sigma_8 = 0.85$ , and nuisance parameters  $\sigma_v = 300$  km/s,  $\sigma_m=0.1$ ,  $\mu_{err} = 0.1$ . We further marginalise over  $M$ .

In Fig 3 we compare the marginalised  $1\sigma$  contours obtained when the coherent PVs are ignored and included, for our hypothetical SNAP and SNfactory surveys. We see that, even for a cut of  $z > 0.03$  the error bars on  $\Omega_m$  and  $w$  will be considerably underestimated if the peculiar velocities are ignored, and in particular the marginalised error on  $w$  increases by 35% from 0.062 to 0.084, for the SNe alone. We therefore conclude that it is essential to include a full covariance matrix analysis at these redshifts, to avoid significantly underestimating the errors. That the error bars increase rather than decrease indicates that the extra information available in the peculiar velocities is outweighed by the extra parameter space  $\{\Omega_b, h, n_s, \sigma_8\}$ .

In light of the extra effort required for the low- $z$  SNe we consider excluding them. However in Fig 3 we see that the contours increase significantly when low- $z$  SNe are not available (marginalised error on  $w$  increase to 0.12), even when CMB data is included. Therefore we conclude that low- $z$  SNe play a vital role in constraining the cosmological parameters, but a full covariance matrix analysis must be done.

We have shown that a low redshift cut of 0.03 is futile in avoiding peculiar velocities when we have 100’s of SNe. We therefore consider that no lower bound on redshift is needed at all, and we extend our study to include SNe with  $z < 0.03$ . We consider a survey of 1000 SNe randomly distributed over 10,000 sq degrees and redshifts

	$w$	$\sigma_8$	$\Omega_m$	$\sigma_v$	$\sigma_m$
A) low- $z$ +PV+BBN+HST	-1	$0.79^{+0.22}_{-0.22}$	$0.48^{+0.30}_{-0.29}$	$275^{+69}_{-70}$	$0.08^{+0.03}_{-0.04}$
B) high- $z$	-1		$0.27^{+0.03}_{-0.03}$	$363^{+169}_{-185}$	$0.12^{+0.02}_{-0.02}$
C) all- $z$ +PV+BBN+HST	-1	$0.78^{+0.23}_{-0.23}$	$0.30^{+0.04}_{-0.04}$	$301^{+53.9}_{-53.4}$	$0.1^{+0.02}_{-0.02}$
D) high- $z$ +WMAP	$-0.96^{+0.09}_{-0.09}$	$0.76^{+0.07}_{-0.07}$	$0.26^{+0.03}_{-0.03}$	$191^{+97}_{-104}$	$0.10^{+0.02}_{-0.02}$
E) high- $z$ +PV+WMAP	$-0.94^{+0.08}_{-0.08}$	$0.75^{+0.06}_{-0.06}$	$0.26^{+0.02}_{-0.03}$	$149^{+107}_{-108}$	$0.11^{+0.02}_{-0.02}$
F) all- $z$ +WMAP	$-0.93^{+0.07}_{-0.07}$	$0.75^{+0.06}_{-0.07}$	$0.26^{+0.02}_{-0.02}$	$395^{+42}_{-42}$	$0.11^{+0.02}_{-0.02}$
G) all- $z$ +PV+WMAP	$-0.86^{+0.08}_{-0.08}$	$0.72^{+0.06}_{-0.07}$	$0.28^{+0.03}_{-0.03}$	$292^{+44}_{-45}$	$0.11^{+0.02}_{-0.02}$
H) WMAP only	$-0.99^{+0.22}_{-0.22}$	$0.76^{+0.09}_{-0.09}$	$0.25^{+0.05}_{-0.05}$		

TABLE I: Mean and 68% confidence limits on the cosmological parameters, and  $\sigma_v, \sigma_m$ , using different combinations of the WMAP and SNe datasets, with and without including the peculiar velocity covariance matrix (PV). See text for discussion.

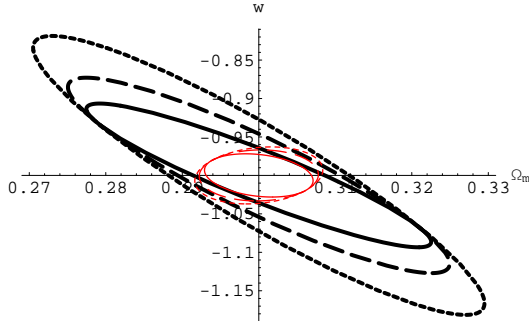


FIG. 3: The marginalised  $1\sigma$  contours for  $\Omega_m$  and  $w$  from a SNAP-like high- $z$  SNe survey in a flat  $\Lambda$ CDM cosmology (short dashed lines). We also consider including 300 low- $z$  SNe from a SNfactory-like survey, while ignoring peculiar velocities (solid lines) and including them (long dashed lines). Smaller red contours include cosmic variance limited CMB, up to  $\ell = 2000$ .

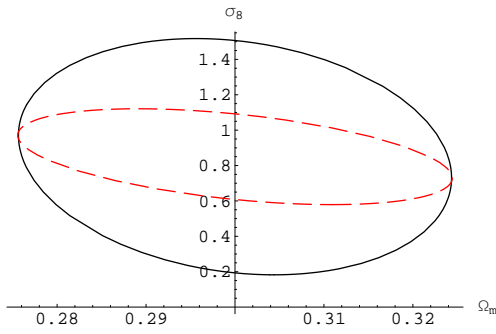


FIG. 4: The marginalised  $1\sigma$  contours for  $\Omega_m$  and  $\sigma_8$ , from 1000 low- $z$  SNe in a  $\Lambda$ CDM cosmology, with  $0.03 < z < 0.08$  (black solid line) and  $z < 0.03$  (red dashed line), combined with a SNAP-like high- $z$  SNe survey.

$z < 0.08$ , and compare it to a similar survey of 1000 SNe, but with  $0.03 < z < 0.08$ . We combine them with a high- $z$  SNAP-like survey as above. In Fig 4 we see that by including very low- $z$  SNe ( $z < 0.03$ ) we have gained

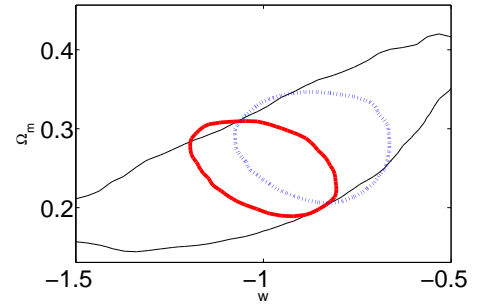


FIG. 2: 95% confidence limits on  $\Omega_m$  and  $w$ , for WMAP only (thin black), WMAP with high- $z$  SNe (thick red), and WMAP with all- $z$  SNe including PVs (dotted blue)

free information about  $\sigma_8$  - ‘free’ because the error bars on  $\Omega_m$  (and  $w$ ) stay the same. However, a lower bound on  $z$  may be useful in reducing the effects of non-linearities.

#### IV. DISCUSSION

We have found that when no redshift cutoff is imposed, the current SNe data detects correlations in PVs at the  $3.6\sigma$  level. We also found that the current constraints on  $w$  are not sensitive to the PVs if SNe with  $z < 0.016$  are excluded. However, we have shown that future large data sets will be sensitive to the PVs even if a lower bound of  $z \geq 0.03$  is used.

An alternative approach of accounting for the correlated peculiar velocities is to estimate the underlying density field from galaxy redshift surveys and then use this to try and remove peculiar velocity at each SNe [21]. As this method has different systematics to the statistical modeling method we have investigated, we believe it will be a useful cross-check to apply both methods separately to future SNe data sets and compare the results.

#### Appendix

For perturbations,  $\rho(1 + \delta)$ , and peculiar velocity  $\mathbf{v}$  we find the perturbed Fourier space continuity equation, in co-moving coordinates, is  $\delta'_{\mathbf{k}} - i\mathbf{k} \cdot \mathbf{v}'_{\mathbf{k}} = 0$  where prime indicates differentiation with respect to conformal time,  $\eta$ . Using the linear approximation  $\delta_{\mathbf{k}}(\eta) = D(\eta)\tilde{\delta}_{\mathbf{k}}$ , and assuming that the Universe has no vorticity ( $\nabla \times \mathbf{v} = 0$ ) leads to  $\mathbf{v}_{\mathbf{k}} = -iD'\frac{\tilde{\delta}_{\mathbf{k}}}{k^2}\mathbf{k}$ , where  $D(z)$  is the growth function. Therefore, the Fourier space correlation between the  $i$ th component of the velocity field at time  $\eta_A$  and the  $j$ th component of the velocity field at time  $\eta_B$  is given by

$$\left\langle v_{\mathbf{k}_A}^i v_{\mathbf{k}_B}^{j*} \right\rangle = D'(\eta_A)D'(\eta_B)(2\pi)^3 \delta(\mathbf{k}_A - \mathbf{k}_B)P(k_A) \frac{k_A^i k_A^j}{(k_A)^4},$$

where  $\langle \delta_{\mathbf{k}_A} \delta_{\mathbf{k}_B} \rangle = (2\pi)^3 \delta(\mathbf{k}_A - \mathbf{k}_B)P(k_A)$ , and the subscripts denote the quantity at time  $\eta_A$  or  $\eta_B$ . This cor-

rects equation (B1) of [31], and our resulting Eq. (5) for  $C_v$  corrects those of [32], among others.

We thank Joe Silk, Pedro Ferreira, and Uroš Seljak for useful conversations. CG is funded by the Beecroft Insti-

tute for Particle Astrophysics and Cosmology, KRL by Glasstone research fellowship and Christ Church college, AS by Oxford Astrophysics. Results were computed on the UK-CCC COSMOS supercomputer.

- 
- [1] A. G. Riess et al. (Supernova Search Team), *Astron. J.* **116**, 1009 (1998), astro-ph/9805201.
  - [2] S. Perlmutter et al. (Supernova Cosmology Project), *Astrophys. J.* **517**, 565 (1999), astro-ph/9812133.
  - [3] P. Astier et al., *Astron. Astrophys.* **447**, 31 (2006).
  - [4] A. G. Riess et al. (2006), astro-ph/0611572.
  - [5] W. M. Wood-Vasey et al. (2007), astro-ph/0701041.
  - [6] G. Aldering et al., in *Survey and Other Telescope Technologies and Discoveries*, edited by J. A. Tyson and S. Wolff (2002), vol. 4836, pp. 61–72.
  - [7] B. Dilday et al., in *Bulletin of the American Astronomical Society* (2005), vol. 37, pp. 1459–+.
  - [8] M. Hamuy et al. (2005), astro-ph/0512039.
  - [9] G. Aldering, *New Astron. Rev.* **49**, 346 (2005).
  - [10] A. G. Riess, W. H. Press, and R. P. Kirshner, *Astrophys. J.* **445**, L91 (1995), astro-ph/9412017.
  - [11] A. G. Riess, M. Davis, J. Baker, and R. P. Kirshner (1997), astro-ph/9707261.
  - [12] I. Zehavi, A. G. Riess, R. P. Kirshner, and A. Dekel, *Astrophys. J.* **503**, 483 (1998), astro-ph/9802252.
  - [13] A. Bonacic, R. A. Schommer, N. B. Suntzeff, and M. M. Phillips, *Bulletin of the American Astronomical Society* **32**, 1285 (2000).
  - [14] D. J. Radburn-Smith, J. R. Lucey, and M. J. Hudson (2004), astro-ph/0409551.
  - [15] C. Bonvin, R. Durrer, and M. Kunz, *Phys. Rev. Lett.* **96**, 191302 (2006), astro-ph/0603240.
  - [16] T. Haugboelle et al. (2006), astro-ph/0612137.
  - [17] S. Jha, A. G. Riess, and R. P. Kirshner, *Astrophys. J.* **659**, 122 (2007), astro-ph/0612666.
  - [18] R. Watkins and H. A. Feldman (2007), astro-ph/0702751.
  - [19] A. Conley et al. (2007), arXiv:0705.0367 [astro-ph].
  - [20] L. Wang (2007), arXiv:0705.0368 [astro-ph].
  - [21] J. D. Neill, M. J. Hudson, and A. Conley (2007), arXiv:0704.1654 [astro-ph].
  - [22] S. Hannestad, T. Haugboelle, and B. Thomsen (2007), arXiv:0705.0979 [astro-ph].
  - [23] L. Hui and P. B. Greene, *Phys. Rev. D* **73**, 123526 (2006), astro-ph/0512159.
  - [24] M. Sasaki, *Mon. Not. Roy. Astron. Soc.* **228**, 653 (1987).
  - [25] N. Sugiura, N. Sugiyama, and M. Sasaki, *Progress of Theoretical Physics* **101**, 903 (1999).
  - [26] T. Pyne and M. Birkinshaw, *Mon. Not. Roy. Astron. Soc.* **348**, 581 (2004), astro-ph/0310841.
  - [27] C. Bonvin, R. Durrer, and M. A. Gasparini, *Phys. Rev. D* **73**, 023523 (2006), astro-ph/0511183.
  - [28] K. Gorski, *Astrophys. J.* **332**, L7 (1988).
  - [29] E. J. Groth, R. Juszkiewicz, and J. P. Ostriker, *Astrophys. J.* **346**, 558 (1989).
  - [30] S. Dodelson, *Modern cosmology* (Academic Press, 2003).
  - [31] C. Hernandez-Monteagudo, L. Verde, R. Jimenez, and D. N. Spergel, *Astrophys. J.* **643**, 598 (2006), astro-ph/0511061.
  - [32] A. Cooray and R. R. Caldwell, *Phys. Rev. D* **73**, 103002 (2006), astro-ph/0601377.
  - [33] L. Silberman, A. Dekel, A. Eldar, and I. Zehavi, *Astrophys. J.* **557**, 102 (2001), astro-ph/0101361.
  - [34] A. Lewis, A. Challinor, and A. Lasenby, *Astrophys. J.* **538**, 473 (2000), astro-ph/9911177.
  - [35] D. J. Eisenstein and W. Hu, *Astrophys. J.* **496**, 605 (1998), astro-ph/9709112.
  - [36] D. Kirkman, D. Tytler, N. Suzuki, J. M. O'Meara, and D. Lubin, *Astrophys. J. Suppl.* **149**, 1 (2003), astro-ph/0302006.
  - [37] W. L. Freedman et al., *Astrophys. J.* **553**, 47 (2001), astro-ph/0012376.
  - [38] A. Lewis and S. Bridle, *Phys. Rev. D* **66**, 103511 (2002).
  - [39] A. Gelman and D. Rubin, *Stat. Sci.* **7**, 457 (1992).
  - [40] T. M. Davis et al. (2007), astro-ph/0701510.
  - [41] D. N. Spergel et al. (WMAP) (2006), astro-ph/0603449.
  - [42] We note that when only weak data are present, the implied priors can have significant effect. In particular, the default `cosmomc` parametrisation is not suitable for our work in absence of CMB or comparably constraining datasets.